IIETA International Information and Engineering Technology Association
Advancing the World of Information and Engineering

Mathematical Modelling of Engineering Problems
Vol. 12, No. 11, November, 2025, pp. 4049-4060
Journal homepage: http://iieta.org/journals/mmep

Design and Experimental Validation of an Optimized FSS Sensor for Wireless Communications

Jagadesh Thirugnanasambantham[1], SatheeshKumar Palanisamy[2*], Singaram Manoharan[1], Sathishkumar Nallusamy[3], Sghaier Guizani[4], Habib Hamam[5,6,7,8]

[1] Department of ECE, KPR Institute of Engineering and Technology, Coimbatore 641407, India
[2] Department of Electronics and Communication Engineering, Alliance School of Applied Engineering, Alliance University, Bengaluru 562106, India
[3] Department of ECE, Sri Krishna College of Engineering and Technology, Coimbatore 641008, India
[4] College of Engineering, Alfaisal University, Riyadh 11533, Saudi Arabia
[5] Faculty of Engineering, Uni de Moncton, Moncton NB E1A3E9, Canada
[6] School of Electrical Engineering, University of Johannesburg, Johannesburg 2006, South Africa
[7] International Institute of Technology and Management (IITG), Libreville BP 1989, Gabon
[8] Bridges for Academic Excellence-Spectrum, Tunis-Centre Ville 1002, Tunisia

Corresponding Author Email: skcommn2@gmail.com

https://doi.org/10.18280/mmep.121131

Received: 5 September 2025
Revised: 30 October 2025
Accepted: 5 November 2025
Available online: 30 November 2025

Keywords:
FSS, SHM, crack detection, electromagnetic sensors, passive wireless sensor, MOEA/D-M optimization algorithm, TE and TM polarization

ABSTRACT

The paper discusses the design, simulation and experimental validation of an optimised Frequency Selective Surface (FSS) sensor in Structural Health Monitoring (SHM) applications. Civil infrastructure is subjected to extreme conditions, including earthquakes and environmental degradation, and requires constant monitoring to ensure structural integrity and reduce the risk of failure. The proposed FSS-based sensor provides a passive, cost-effective method for detecting structural cracks by analysing changes in electromagnetic frequency responses. The sensor is sensitive to the structural changes with a bandwidth of 4 GHz–8 GHz. Several crack cases were modelled in CST Studio, and significant changes in frequency (initialised at 6.07 GHz) were observed depending on the crack's presence, orientation, and size. The FSS construction features a rectangular loop and square patches integrated onto an FR-4 substrate, making it the best performer in TE and TM polarisation modes. The presented design offers superior sensitivity and less acute frequency variations when a crack is present, compared to the current design. To provide angular stability and frequency responsiveness, a multi-objective optimisation algorithm, MOEA/D-M, was used to optimise the FSS parameters. The sensor was experimentally validated in an anechoic chamber using horn antennas and a vector network analyser (VNA), and was shown to detect cracks by measuring changes in resonance frequencies. The findings confirm that the FSS sensor is a highly effective and resilient SHM instrument, providing high-quality, real-time measurements of civil structures under different environmental conditions.

1. INTRODUCTION

A Frequency Selective Surface (FSS) is a passive, periodic structure composed of identical conductive elements arranged in a single unit or a two-dimensional infinite grid. The smallest identical element of any FSS array may comprise one or more elements, known as a unit cell. These unit cells are periodically arranged in a one- or two-dimensional array to form the entire FSS structure. Generally, the unit cell consists of either a conductive patch-type element or an aperture-type element on a dielectric substrate. The incident plane wave is either reflected or transmitted around its resonant frequency. A periodic array can be excited in two distinct ways: either by an incident plane wave (in a passive array) or by connecting a separate voltage source with identical amplitude and phase to each element of the array (in an active array).

Structural Health Monitoring (SHM) has become an essential component in ensuring the longevity and safety of civil infrastructure. Various sensor technologies, such as fiber optics, piezoelectric sensors, and strain gauges, have been employed to monitor the structural integrity of buildings, bridges, and other critical structures. However, these methods often suffer from high cost, complex integration, and maintenance challenges. FSS-based sensors present a passive, wireless alternative that enhances SHM applications by providing a non-intrusive means of detecting structural anomalies through electromagnetic response analysis.

FSS sensors can be embedded within structures to continuously monitor material deformations, load-induced stresses, and crack formations. Their ability to function as

frequency-tuned electromagnetic resonators makes them highly effective in identifying even minor structural changes. Unlike conventional sensors, FSS does not require a power supply for sensing operations, making it a cost-effective solution for long-term SHM. Additionally, their ability to operate in TE and TM polarization modes enhances sensitivity and detection accuracy across a range of environmental conditions.

The deployment of FSS sensors in SHM is justified by their unique ability to detect structural cracks and deformations passively. The resonance frequency of an FSS shifts when physical changes, such as cracks, alter the local dielectric environment. This shift can be analyzed to determine the presence, location, and severity of damage. Traditional sensors require direct contact or embedded wiring systems, whereas FSS-based sensors can be seamlessly integrated into composite materials or applied as surface-mounted structures.

Given the increasing demand for reliable and long-term monitoring solutions, it becomes essential to examine how FSS-based sensing compares with existing SHM approaches. While the work established the functional principles and advantages of FSS sensors, a broader comparison with other established techniques is needed to highlight the specific motivations for adopting FSS in structural monitoring. Such a comparative perspective also clarifies the unique gaps that conventional sensors fail to address, thereby underscoring the relevance of choosing FSS as the sensing framework in this work.

Conventional sensors require direct physical contact or an embedded circuit board, whereas FSS-based sensors can be embedded in composite materials or surface-mounted.

- Fiber Optic Sensors: High sensitivity but costly and challenging to integrate over large surfaces.
- Piezoelectric Sensors: Provide accurate localized measurements but require an external power source and suffer from signal degradation over time.
- Strain Gauges: Simple in design but limited in terms of scalability and environmental resistance.

FSS sensors, on the other hand, offer broadband functionality, polarization stability, and non-contact operation, making them ideal for large-scale monitoring without significant retrofitting costs. They are particularly effective in environments where traditional sensor deployment is difficult, such as high-temperature zones or structures with complex geometries.

The performance of an FSS sensor for SHM is heavily influenced by its geometric configuration and electromagnetic properties. The optimization of FSS parameters—including unit cell dimensions, substrate material selection, and spacing between elements—is crucial for maximizing sensitivity and stability. A multi-objective optimization approach ensures that key performance metrics, such as angular stability, frequency selectivity, and robustness to environmental variations, are simultaneously enhanced.

To achieve this, a multi-objective evolutionary algorithm based on decomposition (MOEA/D-M) is employed to refine FSS designs. This method enhances the trade-offs between competing objectives, such as bandwidth expansion and polarization insensitivity. By leveraging AI-driven optimization techniques, the FSS sensor design can be iteratively improved to achieve higher accuracy in crack detection and better resilience against environmental perturbations.

Additionally, the integration of machine learning models can further improve the detection capabilities of FSS-based SHM systems. By analyzing historical resonance shift data, predictive models can be trained to classify various types of structural anomalies, thereby enabling early-warning systems for infrastructure monitoring.

The main contributions of this work may be summarized as follows:

- Design and Optimization of an FSS-Based SHM Sensor: The development of a novel FSS sensor tailored for SHM, integrating an optimized unit cell geometry for enhanced sensitivity to structural anomalies.
- Integration of Multi-Objective Optimization: Implementation of the MOEA/D-M optimization algorithm to refine key design parameters, achieving improved angular stability, resonance frequency selectivity, and polarization independence.
- Simulation and Experimental Validation: Validation of the proposed FSS sensor through extensive simulations using CST Studio, followed by experimental testing in an anechoic chamber using horn antennas and a vector network analyzer (VNA).
- Electromagnetic Response-Based Crack Detection: Demonstration of the sensor's ability to detect structural cracks via shifts in resonance frequency, enabling passive, non-invasive monitoring of material deformations and stress distributions.
- Comparative Analysis of FSS Geometries: Comprehensive assessment of different FSS unit cell geometries, evaluating their performance in terms of bandwidth, polarization stability, and environmental adaptability.
- Integration with Active Structural Control Systems: Discussion on how FSS-based SHM sensors can be integrated into wireless sensor networks (WSNs), AI-driven predictive maintenance systems, and smart structural materials for real-time monitoring.
- Advancement in Passive Wireless Sensor Technology: Development of an ultra-low-power, maintenance-free sensor that provides reliable long-term SHM capabilities without requiring an external power supply.

2. LITERATURE REVIEW

2.1 Current research

In its simplest form, an FSS functions based on Floquet's principle, which dictates that each unit cell in a planar array should exhibit consistent field and current distributions. Nevertheless, a phase shift may occur between unit cells due to the phase of the incoming wave. When the incident wave encounters the filter, it induces oscillations in the electrons within the metal, influencing wave propagation. The free electrons absorb a large quantity of the incident energy at a certain frequency, causing them to reradiate it in the opposite direction, thereby canceling the initial field and minimizing transmission via the FSS [1].

Various designs have been developed for different applications. The design of an FSS is influenced by several factors, including the angle of incidence of the incoming wave, cross-polarization requirements, and desired bandwidth. The choice of unit cell geometry plays a crucial role in determining electromagnetic characteristics such as resonance frequency, bandwidth, and polarization sensitivity. A thorough analysis

of the techniques used in the creation of frequency-selective surfaces was conducted in the study [2] and also discussed how the size and sensitivity to angle of incidence requirements of current frequency-selective surfaces limit their functionality, demonstrating the need for better qualities. A comparative analysis of different FSS geometries is presented in Table 1.

Table 1. Comparison of various geometries in FSS design

Ref.	Geometry	Bandwidth	Angle Stability	Polarization Sensitivity	Application Suitability
[3]	Jerusalem Cross	Narrow	High	Low	Structural monitoring
[4]	Square Spiral	Wide	Moderate	High	General applications
[5]	Rectangular Loop	Moderate	High	Moderate	Targeted sensor design
[6]	Triangular Patch	Variable	Low	Moderate	Specific frequency tasks
[7]	Circular Elements	Wide	Moderate	High	Versatile applications

Additionally, the implementation of split center resonator (SCR) FSS structures has been explored for enhancing gain performance in various applications. The work presented in reference [8] highlights a gain-enhanced UWB antenna using SCR-based FSS, which optimizes wideband impedance matching while ensuring stable radiation performance. This approach demonstrates the versatility of FSS structures beyond structural monitoring, extending their applicability to high-gain UWB communication systems. By tracking frequency shifts in electromagnetic response brought on by modifications to the structural substrate, the integration of FSS technology into SHM provides a novel method for identifying structural anomalies, such as cracks or deformations. The design and optimization of an FSS-based sensor that can reliably identify and describe structural cracks while preserving broadband operation, polarization stability, and environmental robustness appropriate for monitoring civil infrastructure is thus the main issue this work attempts to address.

2.2 SHM and the role of FSS

SHM is a critical field that ensures the integrity and safety of civil infrastructure. Traditional SHM technologies rely on various sensor types, such as fiber optic sensors [9], piezoelectric sensors [10], and strain gauges. However, these conventional approaches have limitations in terms of cost, integration complexity, and maintenance requirements. FSS-based sensors offer a novel alternative due to their passive operation, adaptability, and electromagnetic response characteristics.

The unique advantage of FSS sensors in SHM lies in their ability to detect structural deformations, cracks, and material degradation through shifts in resonance frequency [11]. The passive wireless nature of these sensors eliminates the need for an external power source, making them a cost-effective solution for long-term monitoring.

Fiber optic, piezoelectric, and strain gauge sensors are examples of traditional SHM methods that have proven to be dependable in detecting localized damage. However, especially for big civil infrastructures subjected to harsh external conditions, these systems frequently have restricted scalability, complicated wiring, and high installation costs. Despite their accuracy, fiber optic sensors need complex interrogation units and are brittle [12]. In a similar vein, the need for active power sources and recurring calibration limits the long-term deployment potential of piezoelectric and strain gauge devices. On the other hand, FSS-based sensors offer a wireless, passive, and affordable substitute that can identify structural abnormalities by measuring changes in electromagnetic resonance, making them a more reliable and long-lasting option for real-time SHM applications.

2.3 Integration of FSS sensors with active structural control systems

- AI-Based Monitoring: Machine learning and AI-driven models can be applied to analyze real-time FSS sensor data, identifying early signs of structural degradation. AI algorithms can predict potential failures by correlating frequency shifts with specific damage patterns, enabling proactive maintenance strategies [13, 14].
- Adaptive Materials and Smart Structures: The integration of FSS sensors with smart materials such as shape memory alloys (SMAs) and piezoelectric actuators can lead to real-time adaptive responses to detected structural changes [15]. For example, upon detection of a frequency shift indicating a crack, piezoelectric actuators can adjust structural tension to mitigate further damage.
- WSNs and IoT Connectivity: By embedding FSS-based SHM sensors into a WSN, real-time data can be transmitted to cloud-based platforms for remote monitoring [16]. This connectivity enhances the efficiency of damage localization, alert systems, and predictive analytics for large-scale infrastructure projects.

2.4 Ability of FSS

FSS-based sensors offer a promising alternative to traditional SHM techniques due to their passive, wireless, and cost-effective characteristics. The ability of FSS to detect structural deformations and cracks via electromagnetic resonance shifts makes it a viable solution for long-term infrastructure monitoring [17]. Furthermore, the integration of FSS sensors with AI-driven monitoring, adaptive materials, and IoT-based networks enhances their capability for real-time structural control [18]. This work explores the design, optimization, and validation of an FSS sensor tailored for SHM applications, emphasizing its feasibility in modern structural control methodologies [19, 20].

2.5 Research gap

Despite significant advancements in SHM and FSS technologies, several challenges remain unaddressed, limiting their practical implementation in real-world infrastructure monitoring. This work aims to bridge the following research gaps:

- Limited Integration of FSS in SHM Applications: While traditional SHM systems utilize fiber optic and

piezoelectric sensors, the potential of FSS-based sensors for passive, wireless, and long-term structural monitoring remains underexplored. Current research lacks practical implementations and comparative studies evaluating FSS against conventional SHM technologies.

- Optimization Constraints in FSS Design: Existing FSS designs often suffer from limited angular stability, resonance frequency drifts, and polarization sensitivity. Although optimization algorithms have been applied in electromagnetic design, the lack of multi-objective optimization frameworks tailored for SHM applications prevents achieving optimal trade-offs between bandwidth, sensitivity, and stability.
- Lack of Experimental Validation in Real-World Scenarios: Many studies focus on theoretical and simulation-based assessments of FSS sensors without extensive experimental validation under real-world conditions. The absence of physical testing limits the understanding of how environmental factors—such as material degradation, mechanical stress, and variable loading—affect sensor performance.
- Inefficient Integration with Smart Structural Control Systems: While AI-driven predictive maintenance models and WSNs are emerging in SHM, there is limited research on integrating FSS-based SHM sensors with these intelligent frameworks. A seamless fusion of FSS with AI-driven analytics could enhance early fault detection and enable automated intervention.
- Electromagnetic Behavior in Complex Structural Materials: The interaction of FSS sensors with heterogeneous and layered structural materials has not been extensively studied. Crack detection efficiency and frequency shift behavior need further exploration, particularly when applied to reinforced concrete, steel structures, or composite materials with varying dielectric properties.

To address the limitations highlighted in the existing literature and bridge the identified research gaps, a systematic methodology is required to develop an FSS-based sensor capable of reliable crack detection. The following section outlines the complete design framework, starting from the geometric modelling of the FSS unit cell to simulation procedures and optimization strategies used to achieve enhanced SHM performance.

3. DESIGN METHODOLOGY

3.1 Design

The design parameters of FSS are resonant frequency, bandwidth, and the configuration of the transmission and reflection curves. These properties collectively depend on a number of variables, including the shape and dimensions of the element, the distance between the elements, the dielectric material in the area, the angle of incidence, and the various polarizations of incoming waves. An FSS element's shape has a significant impact on its bandwidth [21]. The new designed FSS features a single rectangular loop design with square patch integrated at its corners. The frequency response is recorded and the operational frequency is found to be near 6.25 GHz for FSS element on substrate. The substrate is made of FR-4 and is of dimension 13.5 × 13.5 mm and thickness 0.8 mm. The square loop is of length 8 mm. The square patch integrated is of length 3.5 mm and thickness of the conducting element is 0.035 mm shown in Figure 1. The unit cell geometry, including the introduction of square patches at the corners, was carefully chosen through iterative design and simulation to optimize the performance of the FSS. The square patches at the corners provide specific benefits, such as enhancing the angular stability of the FSS and improving its polarization independence. These features ensure better performance across a wider range of incident angles and polarization modes. Additionally, the corner patches contribute to tuning the resonance frequency and achieving the desired frequency-selective behavior, as they influence the overall capacitance and inductance of the unit cell.

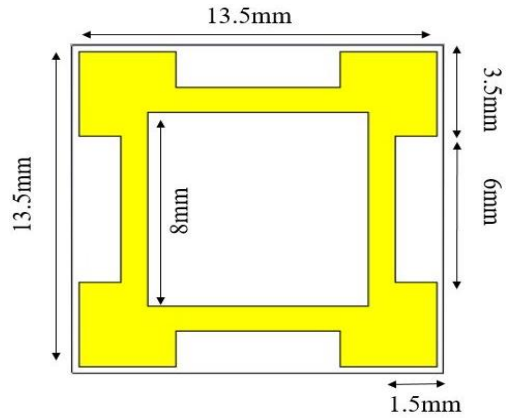

Figure 1. Proposed FSS design

A square loop with a side length of 8 mm, integrated with 3.5 mm square patches at each corner, forms the core resonant structure of the proposed design. The optimized combination of geometric and material parameters ensures consistent resonance performance across the 4–8 GHz frequency band, making the configuration suitable for identifying and monitoring cracks in civil infrastructures.

After conducting several design refinements and electromagnetic simulations using CST Studio Suite, the configuration incorporating corner square patches was finalized. This design enhances the FSS performance by promoting symmetrical current flow and strong capacitive coupling between adjacent unit cells. The addition of corner patches also contributes to improved angular stability and polarization independence, thereby maintaining consistent frequency responses under varying incidence angles and polarization states.

For the simulation environment, periodic boundary conditions were applied along the X and Y directions to emulate an infinite array of unit cells, while open (add space) boundaries were implemented along the Z-axis to represent free-space propagation. A plane wave excitation was used to evaluate the sensor's behavior under both TE and TM polarization modes, with incidence angles ranging from 0° to 60°. These simulation parameters effectively capture the electromagnetic response of the proposed FSS design, ensuring reliable and accurate prediction of its performance under different structural and environmental scenarios.

The sensor showed response at 6.07 GHz within the window of 2–10 GHz. This will be used as reference to compare the response of the FSS sensor with the sample integrated with crack. Both the TE and TM mode showed the same response as shown in Figure 2.

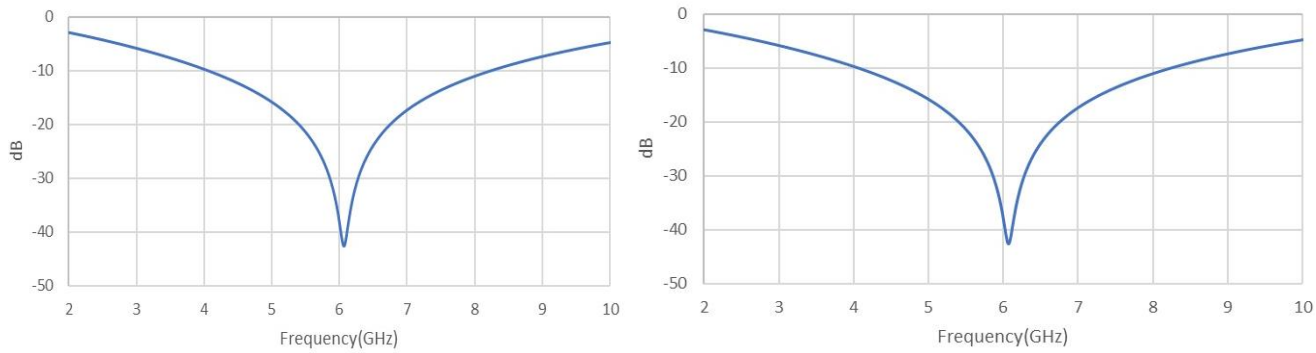

Figure 2. Transmission characteristics in TE and TM mode

3.2 Simulation of cracks

In order to test the sensor for detection of crack, multiple cracks were simulated using CST Studio as shown in Figure 3. The cracks were made up of concrete material of dielectric 5.28. The crack brings change in the dielectric with presence of air gap thus varying the frequency response. The FSS was tested for cracks designed with multiple dimensions.

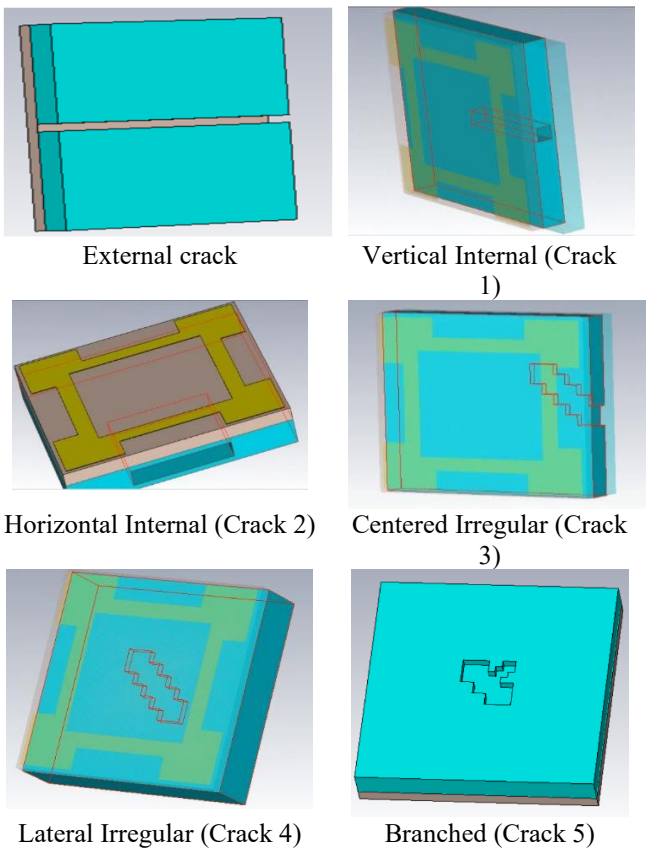

Figure 3. Various types of crack generated in FSS (External, Vertical Internal, Horizontal Internal, Centered Irregular, Lateral Irregular, Branched)

Notes: Concrete; Conducting material; Substrate

The transmission characteristics in TE and TM modes with various types of cracks are shown in Figure 4 and Figure 5. Comparing the frequency response of all the simulated cracks reveals that the sensor exhibits significant variation in the operating frequency range depending on the dimension and position of the crack. The frequency response variation for cracks occurs due to shift in frequency, location and size of cracks and sensor response patterns. The shift that the sensor shows notable fluctuations in the operating frequency range are measured. For the simulated cracks the variation is within the window of 4–7 GHz. The cracks are analysed in both TE as well as in TM mode. The tangential component of the electric field must be continuous across the boundary. This ensures that the fields on opposite sides of the boundary are periodic. The tangential component of the magnetic field must be continuous across the boundary. This ensures that the magnetic field phase changes by a constant amount across the boundary.

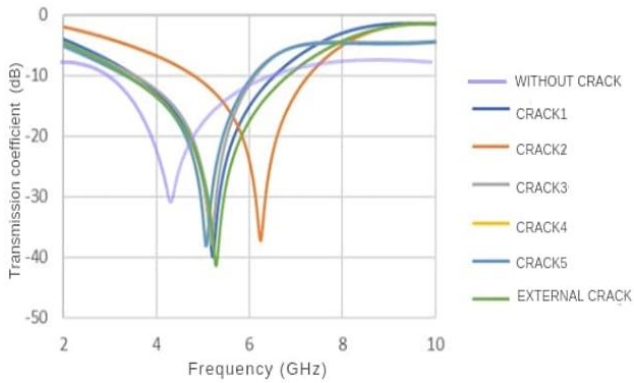

Figure 4. Transmission characteristics in TE mode (with crack)

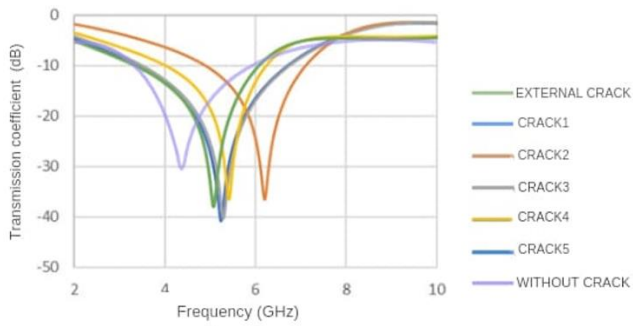

Figure 5. Transmission characteristics in TM mode (with crack)

The designed FSS is polarization insensitive since it responds to both polarization modes (TE and TM) in a nearly identical way. The FSS unit cell is developed for the measurement findings that are obtained. The results of the simulation and measurement coincide well.

The relationship between fracture characteristics and resonant frequency shifts can be better understood by methodically altering crack parameters like as position, depth, and form. A quantitative evaluation of the sensor's sensitivity and capability for precise fracture identification will be made possible by this analysis. Furthermore, experimental validation is essential for verifying the simulation results and proving the sensor's usefulness. The performance of the sensor can be assessed in real-world settings by creating test specimens with controlled fracture shapes and measuring vibration. Strong proof of the sensor's dependability and potential for practical application will be provided by this combined simulation and experimentation method.

3.3 Optimization algorithm for FSS design

A multi-objective optimization problem (MOP) involves finding a vector of decision variables within a specific domain that meets all constraints and optimizes a set of multiple objective functions. These objective functions often consist of subgoals that may conflict with each other. When one subobjective improves, the performance of one or more subobjectives may suffer. That is to say, in order to maximize the optimization of each subobjective, cooperation and compromise amongst them are necessary rather than trying to obtain the ideal values for multiple subobjectives. MOPs are common in real-world scenarios and are often explored in scientific research and practical applications. To address the limitations of existing algorithms, we propose MOEA/D with adaptive exploration and exploitation (MOEA/D-AEE). This algorithm improves global search and adaptive capabilities by using dynamic search and joint development, enhancing sparse distribution and search effectiveness. The approach integrates a joint exploitation coefficient between parent solutions, which helps generate better offspring by adaptively adjusting the relationships between parents and offspring during optimization. Additionally, it utilizes uniformly distributed random integers to explore the solution space more thoroughly, balancing exploration and exploitation. The method actively selects a parent from the original population when two chosen parents are similar, while gradually employing an exploitation strategy to pick a parent from neighbouring solutions when the two selected parents are significantly different. This combination enhances the overall optimization process.

Numerous academics have attempted to use evolutionary algorithms to solve these kinds of issues. Setting weights is the initial step towards turning the two-dimensional problem into a single-objective problem. Nevertheless, the population's distribution is unequal and the basic weighting approach is unable to accurately represent the true state of affairs due to the objective function's increased dimensions. The traditional nondominated genetic sorting algorithm II (NSGA-II) was then proposed by researchers who carried out additional research on the application of multi-objective evolutionary algorithms (MOEAs).

A type of optimization problems known as MOPs are those that have several competing objectives. The purpose of MOP is to acquire a set of optimal solutions that best balance its numerous objectives, as opposed to one optimal solution, as with a single-objective optimization problem (SOP). All possible solutions in the feasible issue area that are independent of other solutions are contained in such an optimal-set Pareto front. The weighted sum method, the Chebyshev method, and the boundary crossing method are common decomposition techniques in this approach. The following is the formula for the most widely used Chebyshev decomposition method:

$$z^* = min(f_1, f_2, \ldots . f_M) \quad (1)$$

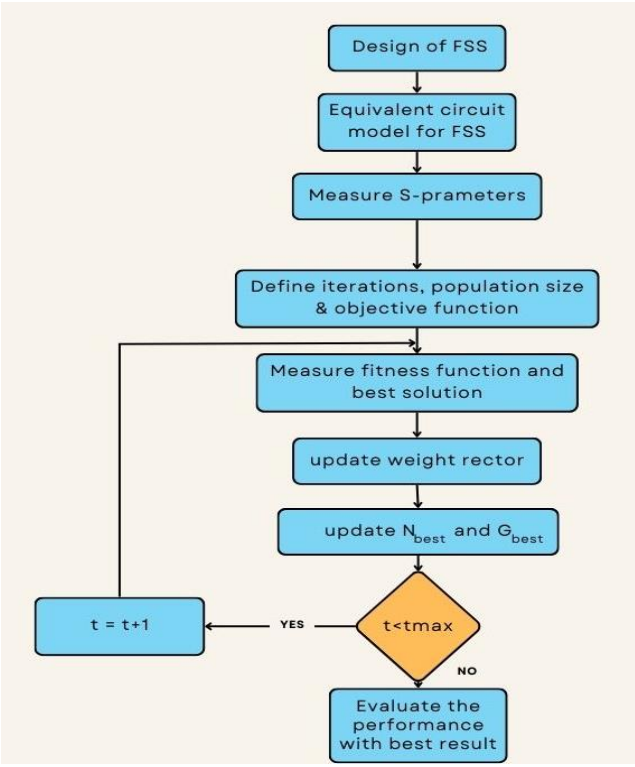

Figure 6. Flowchart of optimization procedure

An improved hybrid optimization method, referred to as MOEA/D-M, is introduced as a sophisticated automated design approach specifically for developing compact FSS antennas. This technique combines the advantages of both particle swarm optimization (PSO) and binary particle swarm optimization (BPSO), integrating them into the structure of MOEA/D. By utilizing group operators in a parallel configuration, the approach improves the search efficiency and precision, offering a more robust solution for optimizing multiple conflicting objectives simultaneously in the antenna design process. This results in a more effective and automated approach to achieving compact and high-performance FSS antennas. During the algorithm's execution, every particle has several neighboring particles, and they are all divided into a few groups. Access to potential or beneficial information is available to members of both groups and communities. Then, within predetermined bounds, MIMO antenna with anticipated performance can be targeted and intelligently generated. In certain MIMO antenna design scenarios, this can serve as an alternative approach. The effectiveness of the design strategy is demonstrated through both single-band and dual-band compact high-isolation FSS antenna designs for SHM applications, which share a common reference model. The proposed method has the potential to significantly enhance the design flexibility of FSS. The figure illustrates the step-by-step optimization process. Figure 6 shows the flowchart of optimization procedure. The detailed procedure of MOEA/D-M is outlined as follows.

While S_{11} is analyzed to understand reflection characteristics, S_{21} provides insight into how effectively the FSS transmits signals. The optimization algorithm may emphasize minimizing the S_{11} parameter to enhance reflection capabilities, it is essential to also consider transmission properties (S_{21}) when discussing overall performance. Both parameters provide a comprehensive view of how the FSS operates within its intended application, particularly in SHM contexts. This dual focus allows for a robust evaluation of both filtering and transmission efficiencies critical for effective sensor design and implementation.

Step 1: Initialization

Construct N weight vectors $\lambda_1,\lambda_2,\ldots.\lambda_N$

Generate initial population through random sampling

Find N_{best} and G_{best}

where N_{best} and G_{best} are the best solution for fitness function and objective value

Initialize $z^*=(z_1^*,z_2^*,\ldots.z_m^*)^T$

where z is objective function or a decision variable within the optimization framework

Set external population=0

Step 2: Reproduction and update

(1) Update weight vector

(2) Revaluate x_i and update F_i for each particle i, where, x_i is individual decision variable or a vector of variables that define a potential solution in the optimization landscape, where, f_i is a fitness value

(3) Update N_{best} and G_{best}

Step 3: Return

The design of FSS is restricted to a predefined to 13.5 mm × 13.5 mm. The evaluation function is given by:

$$f = \frac{1}{h}\sum_{i=1}^{h} \min\,(s_{11}, -10) \tag{2}$$

where, h is the number of sampling points in the operation band and f is the average value of S_{11}.

Furthermore, multi-objective functions are defined as follows:

$$f_1 = \frac{1}{h}\sum_{i=1}^{h} \min\,(s_{11}, -10) \tag{3}$$

$$f_2 = \frac{1}{h}\sum_{i=1}^{h} \min(s_{11}, -15) \tag{4}$$

The performance evaluation of the optimized FSS design with the literature is presented in Table 2. The suggested FSS's unit cell size is optimized through the use of the MOEA/D-M algorithm, ensuring a 60° angular stability.

Table 2. Performance evaluation of optimized FSS design

Ref.	Size of FSS (λ_o)	Operating Band (GHz)	Angular Stability	Polarization
[7]	1.1 × 1.1	5.6	60°	Dual
[4]	0.9 × 0.9	6.8	45°	Not reported
[17]	0.67 × 0.67	5.3	60°	Dual
[18]	0.5 × 0.5	4.8	60°	Dual
This work	0.38 × 0.38	6.2	60°	Dual

Achieving the best possible balance between convergence precision and computing economy was the main focus of the algorithm's parameter setting. In order to maintain feasible computing effort and guarantee sufficient coverage of the design space, a population size of 10,000 was chosen. In order to attain steady convergence for both goals—reducing reflection loss and improving angular stability—the optimization procedure was carried out for 1,500 generations.

The crossover and mutation probabilities were chosen at 0.9 and 0.1, respectively, to preserve diversity within the evolving population and avoid early stagnation. Using uniformly distributed weight vectors, the multi-objective optimization challenge was broken down into several scalar subproblems, each of which was able to reflect a distinct trade-off between the objectives. In order to improve the algorithm's capacity to converge effectively toward the Pareto-optimal front and guarantee a fairly distributed collection of optimal design solutions, information exchange between nearby solutions was also included.

4. RESULTS

4.1 Fabrication and validation

The sensor is fabricated with FR-4 as substrate of dielectric constant 5.28 and Copper as the conducting element shown in Figure 7. The FSS sensor has a thickness of 0.8mm. The metallic component is fabricated on one side of the substrate surface and is symmetric in nature. The total

dimension of the sensor is 300 × 300 mm with 21 unit cell in each row and column. Simulation results are portrayed only for a single unit cell, with the simulated crack fitting within the unit cell. But behaviour of a sensor with 21 × 21 unit cells has been illustrated with measurement results.

4.2 Testing

The testing of the sensor is conducted within closed environment. The setup includes anechoic chamber with Horn antennas and VNA, as shown in Figure 7. The FSS sensor's location was where the horn antenna was positioned during the testwith a distance of 1 metre. Reflection measurements were conducted using a bistatic configuration, where one horn provided the excitation signal and another received the reflected response. The receiving horn was connected to a calibrated port of an N9951B Field Fox Handheld Microwave Analyzer for measurement purposes. A Floquet port is a specialized boundary condition used in electromagnetic simulation software, particularly for analyzing periodic structures. Since FSS is a periodic structure, Floquet port is used for simulation. The proposed FSS design is along x and y directions and z-direction is set to be open for free space. The tangential component of the electric field must be continuous across the boundary. This ensures that the fields on opposite sides of the boundary are periodic. The tangential component of the magnetic field must be continuous across the boundary. The sweep settings of VNA is having frequency range of 4 GHz to 8 GHz with 1001 sweep points and linear sweep type having IF bandwidth of 100 Hz.

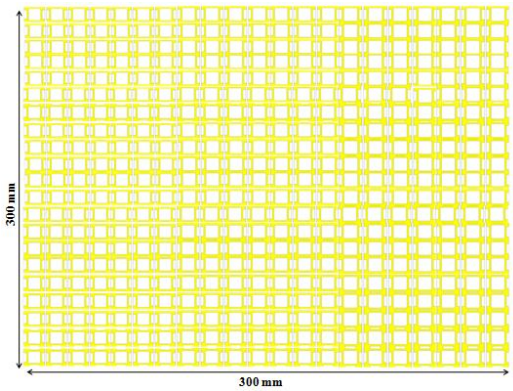

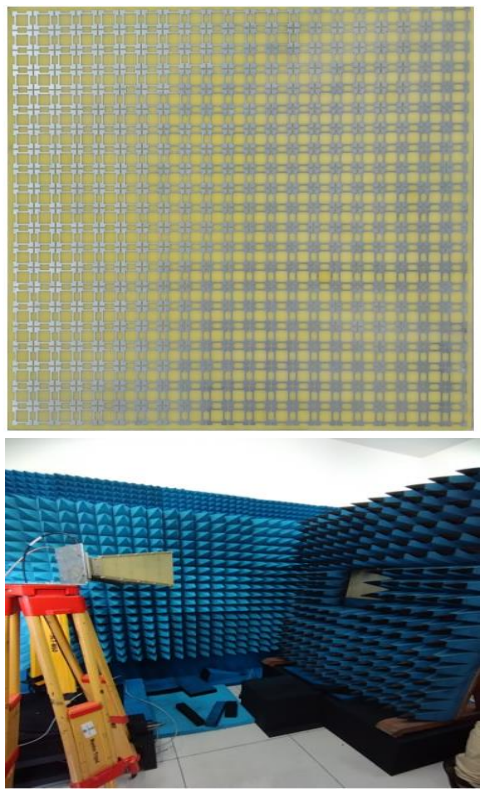

Figure 7. Fabricated FSS and measurement setup

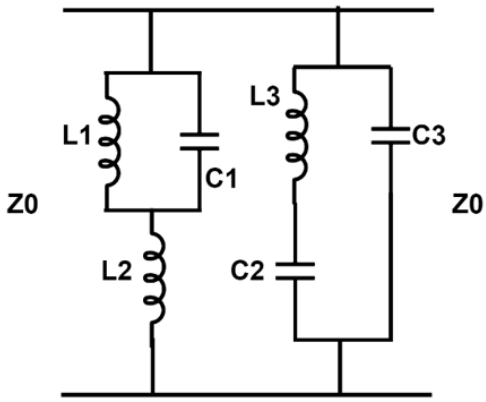

Figure 8. Equivalent circuit model of FSS

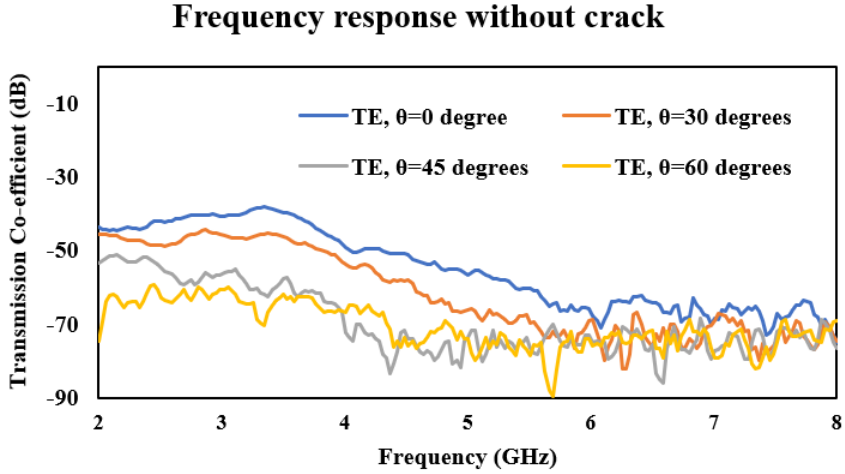

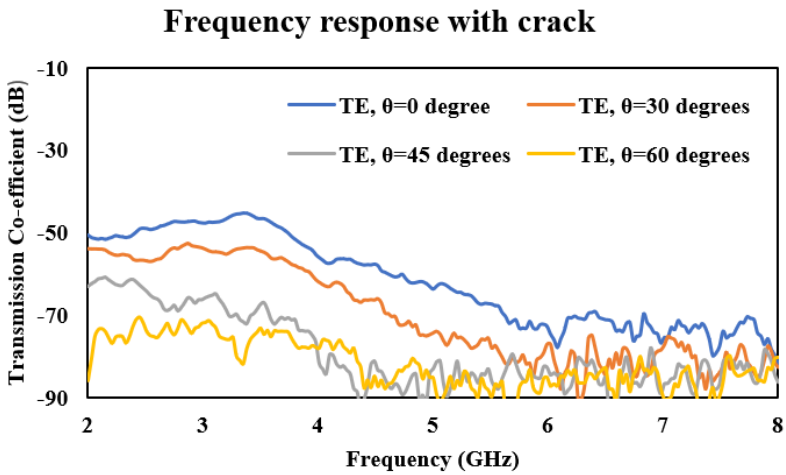

Figure 9. Transmission characteristics at various incident angle (with and without crack–Scenario-I)

Figure 10. Tile with crack

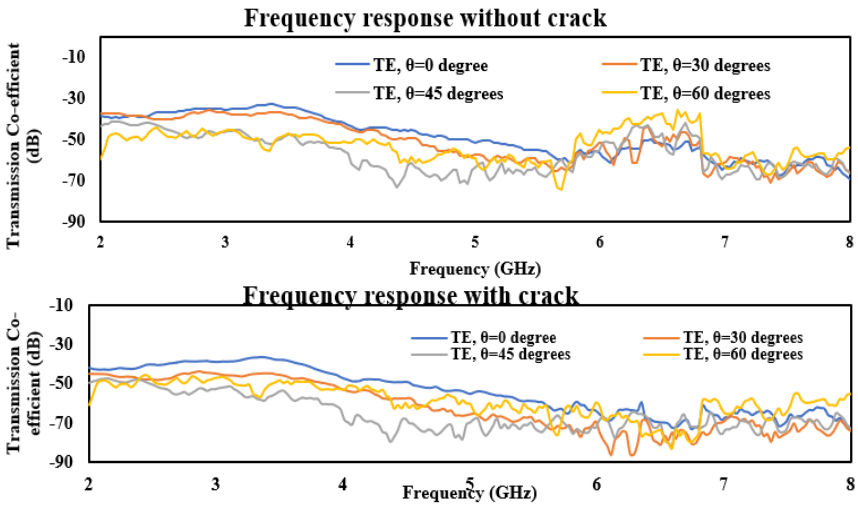

Figure 11. Transmission characteristics at various incident angle (with and without crack–Scenario-II)

The equivalent circuit of the proposed FSS is shown in Figure 8 with L_1=28 mH, L_2=1.6 mH, L_3=1.33 mH, C_1=0.9 nF, C_2=1.44 µF and C_3=3.6 nF obtained at 6.07 GHz. For measurement of the Transmission characteristics one of the Horn antenna is placed behind the FSS sensor. The testing of the FSS included measuring the frequency response of the sensor, sensor when adhered with tile without crack and for a tile with crack shown in Figure 9. Figure 10 shows the tile with crack. Also, the response was recorded for various incident angle of 0°, 30°, 45°, 60°, as shown in Figure 11.

After observation it is found that the operating frequency shifts from 6.76 GHz to a larger value of 7.56 GHz in the presence of crack in tile for incident angle of 60°. It is clear that there exists shift in operating frequency on introduction of crack as shown in Figure 12. Figure 13 shows the Surface Current Distribution at 7 GHz.

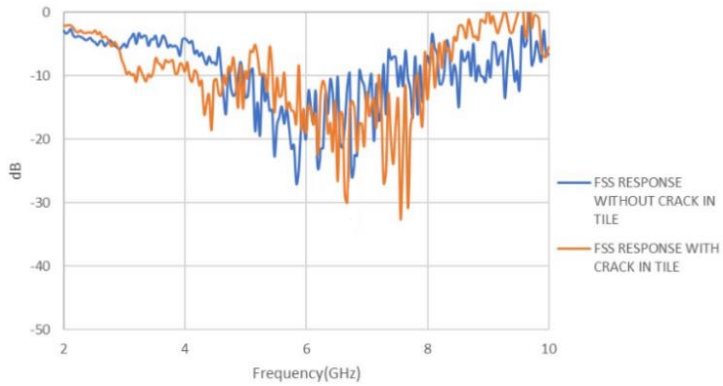

Figure 12. Transmission characteristics of tile with and without crack (Measured)

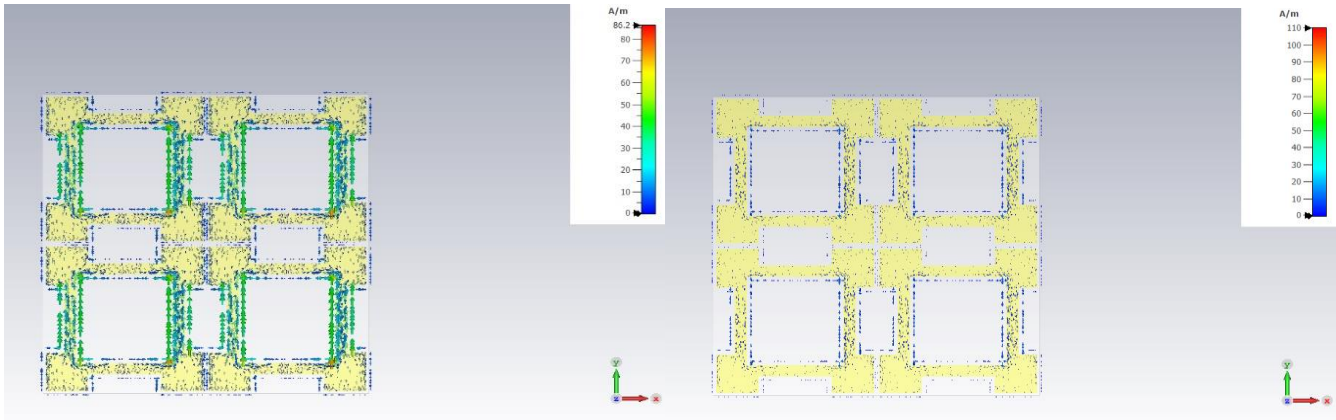

Figure 13. Surface current distribution at 7 GHz

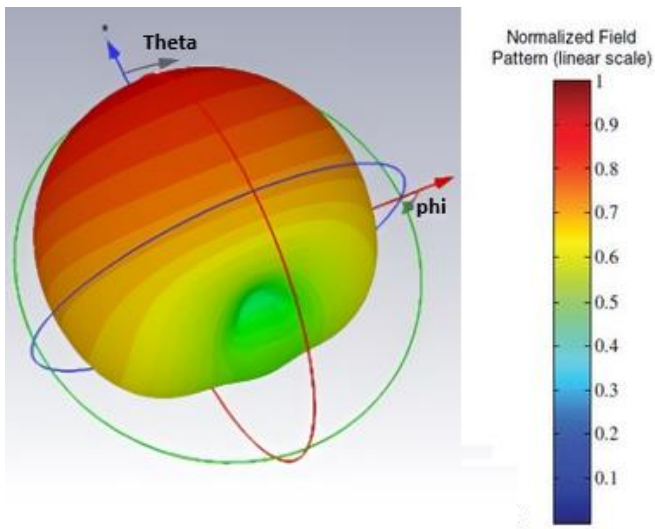

Figure 14. 3D pattern of the proposed FSS

An FSS-based sensor's sensitivity is directly impacted by the resonance frequency shift, which is greatly influenced by the depth of a crack. Deeper cracks change the local dielectric characteristics and interfere with the flow of current across the FSS surface. The resonance frequency shifts noticeably as a result of this modification in the resonant structure's effective capacitance and inductance.

Deeper cracks typically cause bigger disruptions in the electromagnetic coupling between nearby resonant parts, which results in more noticeable frequency shifts. Shallow cracks, on the other hand, only cause slight frequency variations that might be near the detection limit of the device. Thus, the degree of frequency shift (Δf) can be measured as a way to assess how serious structural fissures are. Figure 14 shows the 3D pattern of the proposed FSS.

The testing of the sensor is conducted within a closed environment. The setup includes an anechoic chamber with Horn antennas and VNA. For the test, the horn antenna was placed at the location of the FSS sensor. Reflection measurements were made in a bistatic setup, meaning that one horn was used to provide the excitation signal, and a second (identical) horn was used to receive the reflection response

from the sensor Measurements were made by connecting the receiving horn antenna to a calibrated port of an N9951B FieldFox Handheld Microwave Analyzer. One Horn antenna is placed behind the FSS sensor to measure the transmission characteristics. Think about a cantilever beam that has a crack in the middle. According to the simulation results, as the fracture depth rises, the FSS sensor's resonance frequency will vary significantly. Quantitative data, such as S-parameter measurements, can be used to compare simulated and measured results, allowing for a rigorous evaluation of the FSS's performance. By discussing potential sources of error in both simulations and experiments, the accuracy of the results can be assessed. Clear and concise visualizations, such as graphs and figures, can facilitate a visual understanding of the differences and similarities between simulated and measured results. By incorporating these suggestions, the Fabrication and Validation section can provide a more robust and convincing demonstration of the FSS's performance, strengthening the overall impact of the research.

A number of tests are carried out on beams with different crack depths in order to verify this. The sensitivity of the FSS sensor to crack damage is confirmed by the experimental results, which accord well with the calculations. The features of the structure cause a shift in the FSS's resonance frequency. The possibility of employing FSS sensors for fracture detection in SHM is illustrated by this case study. A precise and non-invasive fracture detection method can be accomplished by utilizing the FSS's sensitivity to modifications in the structural characteristics. More investigation is required to improve the FSS design.

The collective simulation and experimental findings confirm the sensor's capability to detect crack-induced variations in structural materials. These insights form the basis for the broader implications of this work, which are summarized in the concluding section. The conclusion also outlines the limitations of the current study and highlights the pathways for future enhancement of FSS-based SHM systems.

5. CONCLUSION

5.1 Recapitulation

This study presented the design, simulation, and experimental validation of a FSS based sensor for SHM. The sensor was developed to operate within a frequency range of 2 to 10 GHz, with simulations confirming its sensitivity to structural cracks through measurable shifts in resonance frequency.

In simulation tests, the frequency response of the sensor was recorded under multiple crack scenarios, demonstrating a frequency shift in the range of 4–8 GHz due to crack formation. The fabricated sensor was experimentally validated in a laboratory environment using horn antennas and a VNA in an anechoic chamber. The experimental results revealed a frequency shift from 6.28 GHz to 7.56 GHz, supporting the hypothesis that crack-induced changes in the effective periodic element size influence resonance behavior. This work is limited, though, in that the validation was only done inside the anechoic chamber, and the sensor's performance in a real-time setting was not assessed.

Although the study establishes the feasibility of the FSS sensor for SHM applications, further validation is required to confirm the direct correlation between crack dimensions and frequency shifts. Additional testing is needed to refine the understanding of how variations in periodic element dimensions affect resonance under real-world conditions.

Future research will investigate sophisticated FSS geometries, such as fractal and multi-resonant structures, to improve bandwidth, sensitivity, and polarization stability. For real-time SHM, research will also concentrate on creating scalable and modular sensor arrays that can be deployed over wide areas of buildings and bridges in conjunction with low-power wireless interrogation systems. It is anticipated that these advancements would transform the suggested design from a lab prototype into a reliable and field-ready sensing system for real-world civil infrastructure applications.

5.2 Future work

While the current research demonstrates the potential of FSS-based sensors for crack detection, several aspects warrant further exploration:

- Extended Experimental Validation: Additional tests should be conducted under real-world structural conditions to assess environmental influences such as temperature variations, material heterogeneity, and long-term durability.
- Optimized Design for Enhanced Sensitivity: Future work could investigate alternative FSS geometries and substrate materials to further enhance sensitivity, reduce fabrication costs, and improve robustness in harsh environments.
- Angle of Incidence Sensitivity Analysis: Although slight variations were observed, a deeper analysis is necessary to quantify and mitigate angle dependency, ensuring the sensor remains effective across diverse structural orientations.

By addressing these challenges, future research can refine the sensor's reliability, scalability, and integration into modern SHM frameworks.

REFERENCES

[1] Zhou, Y.J., Wu, X.B., Cai, X.D., Xu, H.X., Li, Q.Y., Xiong, W., Xiao, S.Y., Cui, T.J. (2025). Smart meta-device powered by stray microwave energies: A green approach to shielding external interference and detection. Applied Energy, 378: 124770. https://doi.org/10.1016/j.apenergy.2024.124770

[2] Afzal, W., Baig, M.Z., Ebrahimi, A., Robel, M.R., Rana, M.T.A., Rowe, W. (2024). Frequency selective surfaces: Design, analysis, and applications. Telecom, 5(4): 1102-1128. https://doi.org/10.3390/telecom5040056

[3] Wang, Q., Chen, L., Xiao, G., Wang, P., Gu, Y., Lu, J. (2024). Elevator fault diagnosis based on digital twin and PINNs-e-RGCN. Scientific Reports, 14(1): 30713. https://doi.org/10.1038/s41598-024-78784-7

[4] Mahmoodi, M., VanZant, L., Donnell, K.M. (2020). An aperture efficiency approach for optimization of FSS-based sensor resolution. IEEE Transactions on Instrumentation and Measurement, 69(10): 7837-7845. https://doi.org/10.1109/TIM.2020.2986108

[5] Sathishkumar, N., Palanisamy, S., Natarajan, R., VR, A., Ouahada, K., Hamam, H. (2024). Experimental investigations of dual functional substrate integrated waveguide antenna with enhanced directivity for 5G

mobile communications. Heliyon, 10(17): e36929. https://doi.org/10.1016/j.heliyon.2024.e36929
[6] Lu, Y., Wang, S., Zhang, C., Chen, R., Dui, H., Mu, R. (2024). Adaptive maintenance window-based opportunistic maintenance optimization considering operational reliability and cost. Reliability Engineering & System Safety, 250: 110292. https://doi.org/10.1016/j.ress.2024.110292
[7] Arif, B., Bilal, M., Quddus, A., Saleem, R., Ouahada, K., Rehman, A.U. (2024). A split center resonator FSS-based gain enhancement of CPW feed UWB antenna for high gain UWB communication. IEEE Access, 12: 73247-73257. https://doi.org/10.1109/ACCESS.2024.3403719
[8] Soman, R., Wee, J., Peters, K. (2021). Optical fiber sensors for ultrasonic structural health monitoring: A review. Sensors, 21(21): 7345. https://doi.org/10.3390/s21217345
[9] Ju, M., Dou, Z.S., Li, J.W., Qiu, X.T., Shen, B.L., Zhang, D.W., Yao, F.Z., Gong, W., Wang, K. (2023). Piezoelectric materials and sensors for structural health monitoring: Fundamental aspects, current status, and future perspectives. Sensors, 23(1): 543. https://doi.org/10.3390/s23010543
[10] Wang, X., Shi, K.X., Wang, J.L., Jia, Z., Wang, Z.L., Sun, Z.S., Fan, B. (2023). Flexible strain sensor based on a frequency selective surface. Optics Express, 31(5): 8884-8896. https://doi.org/10.1364/oe.484934
[11] Palanisamy, S., Nallusamy, S., Thangavelsamy, N., Guizani, S., Hamam, H. (2025). High-performance sub-6GHz 5G antenna with frequency selective surface integration: Design, optimization and experimental validation. Traitement du Signal, 42(4): 1823-1839. https://doi.org/10.18280/ts.420401
[12] Tütüncü, B., Kartal, M.E. (2025). Design and experimental validation of a compact FSS-based absorber for sub-6 GHz 5G applications. Physica Scripta, 100(10): 105519. https://doi.org/10.1088/1402-4896/ae0f62
[13] Ma, S.N., Xu, Y.P., Pang, Y.X., Zhao, X., Li, Y.F., Qin, Z.G., Liu, Z.J., Lu, P., Bao, X.Y. (2022). Optical fiber sensors for high-temperature monitoring: A review. Sensors, 22(15): 5722. https://doi.org/10.3390/s22155722
[14] Kanchana, D., Radha, S., Sreeja, B.S., Manikandan, E. (2020). A single layer UWB frequency selective surface for shielding application. Journal of Electronic Materials, 49: 4794-4800. https://doi.org/10.1007/s11664-020-08210-x
[15] Cao, H., Thakar, S.K., Oseng, M.L., Nguyen, C.M., Jebali, C., Kouki, A.B., Chiao, J.C. (2015). Development and characterization of a novel interdigitated capacitive strain sensor for structural health monitoring. IEEE Sensors Journal, 15(11): 6542-6548. https://doi.org/10.1109/JSEN.2015.2461591
[16] Kim, M.S., Heo, J.K., Rodrigue, H., Lee, H.T., Pané, S., Han, M.W., Ahn, S.H. (2023). Shape memory alloy (SMA) actuators: The role of material, form, and scaling effects. Advanced Materials, 35(33): 2208517. https://doi.org/10.1002/adma.202208517
[17] Guan, Y.M., Yang, L.Q., Chen, C., Wan, R., Guo, C., Wang, P.F. (2025). Regulable crack patterns for the fabrication of high-performance transparent EMI shielding windows. iScience, 28(1): 111543. https://doi.org/10.1016/j.isci.2024.111543
[18] Suganya, E., Prabhu, T., Palanisamy, S., Salau, A.O. (2024). Design and performance analysis of L-slotted MIMO antenna with improved isolation using defected ground structure for S-band satellite application. International Journal of Communication Systems, 37(16): e5901. https://doi.org/10.1002/dac.5901
[19] Palanisamy, S., Vaddinuri, A.R., Khan, A.A., Faheem, M. (2024), Modeling of inscribed dual band circular fractal antenna for Wi-Fi application using descartes circle theorem. Engineering Reports, 7(1): e13019. https://doi.org/10.1002/eng2.13019
[20] Yang, J.X., Li, H., Zou, J.Z., Jiang, S.X., Li, R., Liu, X.L. (2022). Concrete crack segmentation based on UAV-enabled edge computing. Neurocomputing, 485: 233-241. https://doi.org/10.1016/j.neucom.2021.03.139
[21] Huang, Z.L., Zhang, C.X., Ge, L.Y., Chen, Z., Lu, K., Wu, C.Z. (2024). Joining spatial deformable convolution and a dense feature pyramid for surface defect detection. IEEE Transactions on Instrumentation and Measurement, 73: 1-14. https://doi.org/10.1109/TIM.2024.3370962